

Unveiling an additively manufactured open hardware pin-on-disc tribometer considering its high reproducibility

Christian Orgeldinger^{*}, Tobias Rosnitschek, Stephan Tremmel

Engineering Design and CAD, University of Bayreuth, Universitätsstr. 30, 95447 Bayreuth, Germany

ARTICLE INFO

Keywords:

Pin-on-disc tribometer
Open hardware
Additive manufacturing
Metrology

ABSTRACT

In recent years, the aspects of energy efficiency and durability have become increasingly important in the development of technical systems. From a tribological point of view, these are often linked to the reduction of wear and friction. When testing new materials, coating systems or lubricants, the underlying mechanisms and physical relationships are investigated by the deployment of simplified model tests. Advanced commercial test rigs allow high-resolution measurement of important friction and wear parameters, but also entail a considerable cost and thus a certain entry barrier to deal further with tribological aspects. In many research projects, therefore, self-developed test rigs are used, which at the same time, however, makes comparability and reproducibility with other systems considerably more difficult. For this reason, we have developed a pin-on-disc tribometer based on the open hardware approach, which can be completely additively manufactured by fused filament fabrication. In addition to presenting the customizable measurement system, we investigated the measurement capability using 50 repeated measurements on two different tribological test systems. The reproducibility of the measured values was 0.4 % and 1.1 % for friction and 0.6 % and 1.0 % for wear and was thus considerably lower than the standard deviation in the tests on a single tribometer, which was up to 7.7 % and 16.1 % for friction and wear, respectively. So, the presented tribometer can be used, for example, to perform high throughput tests and thus to detect systematic correlations, e.g., in combination with machine learning approaches. Another area of application is training and education of students and professionals.

1. Introduction

To achieve the necessary transition to global climate neutrality in the next few years, it is becoming increasingly important to focus on aspects of sustainability and energy efficiency of subsequent products right from the start of product development. These include, for example, the availability and recyclability of the materials used, a product design that is as durable as possible, and the lowest possible energy consumption throughout the entire product life cycle. Looking at the tribological aspects of products, energy consumption is directly linked to reduced friction and product longevity to wear. If one considers the share of tribological contacts in total global energy consumption, it is enormous. Holmberg and Erdemir assume that almost a quarter of the energy is attributed to tribological contacts [1]. They further suppose that friction- and wear-induced losses could be reduced by around 40 % in the long term, whereby they see the greatest potential in the short term in transportation and power generation.

To be able to exploit this potential, companies where tribology is not

part of their core business must have the appropriate know-how and equipment in their development departments. If tribological improvements, such as coatings or new material pairings and lubricants, are to be investigated, simple model tests are usually the first step [2]. However, since real tribocontacts are much more complex, an immediate transfer of the findings is often only possible to a limited extent, but they are still suitable for an initial assessment and have thus become established as a quasi-standard. Among these, pin-on-disc or ball-on-disc tribometer tests are particularly widespread due to their simple design. Based on their wide range of application and high relevance, their use is found in standards such as ASTM G99-17 [3] for wear measurement or modified to a linear reciprocal relative motion in ASTM G133-05 [4]. Although withdrawn, DIN 50324:1992-07 [5] is also often deployed to describe the test setup. International ISO 18535:2016 [6] describes the ball-on-disc setup specifically for characterizing the friction and wear behavior of DLC coatings. Similar test setups are relevant in other applications, such as for determining the wear of polymer materials in prostheses according to ASTM F732-17 [7].

^{*} Corresponding author.

E-mail address: christian.orgeldinger@uni-bayreuth.de (C. Orgeldinger).

<https://doi.org/10.1016/j.wear.2024.205437>

Received 14 March 2024; Received in revised form 3 June 2024; Accepted 5 June 2024

Available online 11 June 2024

0043-1648/© 2024 The Authors. Published by Elsevier B.V. This is an open access article under the CC BY-NC license (<http://creativecommons.org/licenses/by-nc/4.0/>).

Based on the standards, there is now a wide range of commercial tribometers with which pin-on-disc tests can be carried out with the highest demands on measurement uncertainty. This is particularly necessary when very fine differences, e.g., in batches, must be determined, or for tests with very small friction forces at the micro and nano level. However, for fundamental investigations such as a comparison of different coating systems or lubricants with frequently used moderate contact forces and at room temperature, the requirements on the measuring system and the test setup are sometimes many times exaggerated. In addition, the high acquisition costs in smaller companies and institutes, as well as in underfunded research units, can represent an inhibition threshold for tribological investigations. Consequently, self-developed test rigs are often used in the literature for pin-on-disc tests as e.g., in Refs. [8–10]. According to Zhou et al. [11] these are used in about one third of all publications of the most important tribology journals. Furthermore, by customizing to the tests to be performed, special test conditions such as tests under vacuum conditions [12,13] or under high temperatures [14] can be realized for which no or not sufficiently adaptable commercial solutions may be available.

Although self-developed test rigs are commonly used, their specifications are usually only mentioned in the respective "Material and Methods" section. A detailed description of the test rig, on the other hand, is rarely given. A detailed description of development, design and construction can sometimes be found in student projects and theses [15–17]. A design concept for a circular and linear tribometer test can be found in Marjanovic et al. [18]. A test rig for biomedical application following ASTM F732-17 was presented by Joyce [19]. Mohan et al. [20] presented development and design for a linear tribometer. Comparatively detailed, Ochs and Victoria [21] presented the design of a pin-on-disc tribometer from a student project. Another multifunctionally tribometer was presented by Chen et al. [22]. With a focus on low cost, Singh et al. [23] presented a tribometer controlled by an ARDUINO™ microcontroller. A linear tribometer with different design concepts was presented by Alvizo et al. [24]. For reciprocating tests under high contact pressures, Berglund et al. [25] presented a test rig. A pin-on-disc test rig for rotary motion based on the current international standards was developed by Hidalgo et al. [26]. Finally, a tribometer for particularly high precision was presented by Lyashenko et al. [27].

Going one step further, open hardware-based concepts have become increasingly popular in recent years in a wide variety of fields and have made an important contribution to free and open science. Although a fully open concept lends itself very well to tribometers due to their simple design, only a few freely available test rigs exist in this area. For example, De Faria et al. [28] presented an open source-based tribometer for linear motion whose design is based on additively manufactured components. The work of Zhou et al. [11] is also particularly worth mentioning at this point. In their publication, the authors presented an open source tribometer and were also able to show that it can be used to achieve highly reproducible measurements.

The subject of measurement uncertainty is of decisive importance in this context but is neglected in many studies. Overall, the test rigs developed can be considered suitable if the measurement uncertainty in the results from the test setup is sufficiently smaller than the differences between the repeated tests. An exact determination of the measurement uncertainty is extremely difficult due to the many different influences on the measurement process. For this reason, there is no uniform metrological traceability in the field of tribological testing technology, as is the case, for example, in length and mass measurement technology. At the same time, the test setup in tribometer tests directly influences the variable to be measured, which is why there is no metrologically traceable standard as in the aforementioned disciplines. Therefore, from a metrological point of view, a tribological measurement is, strictly speaking, always just a test, even if the terms are often used equivalently. In tribological measurement technology, a measurement system analysis can therefore only provide conclusions about the precision, but never about the accuracy of the system. An estimate of the repeatability

and reproducibility of tribological tests can be made, for example, by Round Robin tests (e.g., according to ASTM E691-11 [29]), as carried out by Czichos et al. [30,31] for dry-running ball-on-disc tribometer tests at different institutes and under conditions that are as identical as possible. The resulting coefficients of friction (COF) and wear rates were evaluated. The repeatability of the friction measurement was at best $s_f = \pm 9\%$ within one laboratory and the reproducibility $s_R = \pm 18\%$ between different laboratories, with deviations in system wear being even significantly higher [32]. Another Round Robin test for tribological tests in translatory oscillation apparatus was evaluated by Woydt and Ebrecht [33]. Systematic studies of measurement uncertainty on a single test rig can be found, for example, in Goldstein [34] for a universal tribometer or in Liguori et al. for a linear ball-on-disc tribometer [35,36] and in comparison, with a continuous sliding pin-on-disc test [37]. Ruggiero et al. [38] also investigated COF determination. Dynamic effects on the measurement were investigated by Godfrey [39] or Prost et al. [40] on rotating pin-on-disc tribometers, among others. Do Vale and Da Silva [41] investigated measurement uncertainty for a journal bearing test rig. Particularly noteworthy at this point is the work of Novak and Polcar [42], who dealt in detail with the determination of measurement uncertainty in pin-on-disc tribometer tests on thin films and discussed possible influences. In doing so, the authors followed the international standard for measurement uncertainty determination according to GUM [43]. The operator evaluating the wear therefore had a particularly large influence on the wear rate. Misalignment of the pin and sample, on the other hand, was negligible compared to other sources of uncertainty in the test rig. It should be noted that the minimum and maximum measured values are better suited for describing the variance than the standard deviation and that the uncertainty should always be increased with a coverage factor. The uncertainty of the friction due to the variance is therefore higher than the instrument uncertainty. Individual tests should never be used in tribological measurements. Schmitz et al. investigated the uncertainty in the wear rate [44] and in friction [45] for a linear tribometer. With regard to the wear rate, the greatest influence by far on the uncertainty was determined in the test setup there by measuring the sample mass before and after the test. Relevant influences on the friction measurement were therefore, for example, the calibration of the force sensors used, a deviation of the sensor axis and the deviations in the voltage measurements. Based on this, further work was done on measurement uncertainty in tribometer tests [46–48]. A mathematical approach to correct measurement errors that arise was presented by Sheng et al. [49]. Since uncertainty is of crucial importance in force measurement, it should be calibrated in a traceable manner. Bhattacharjee et al. [50], for example, presented a method of how this can be achieved for friction measurement using atomic force microscopy.

In addition to the uncertainties from the measurement itself, the uncertainties from the subsequent evaluation, e.g., of the wear trace [50, 51], may also have to be taken into account. This is particularly important for measuring the wear track, as the measurement of surface topographies is always subject to measurement uncertainties, depending on the method used [52]. The shape of the wear track, for example, can have an influence on the accuracy and precision of the volumetric wear measurement [53] and especially for small amounts of wear, where the wear track appears to be lost in the surface roughness, the use of the processing algorithms, as in Genta and Maculotti [54], is of decisive importance.

A comprehensive overview of the possible errors and limitations of profilometric measurement of wear in various tribological tests can also be found from Pawlus und Reizer [55]. For very small wear volumes in the order of magnitude of the asperities, the difference measurement of the surface profile is also possible, but then uncertainties due to the repositioning must be considered [56].

For these reasons, it seems important to specify the measurement system used, the exact evaluation and, if possible, a measurement uncertainty, to make the tests performed as reproducible as possible.

Within the scope of our work, we have developed an open hardware-based tribometer whose specifications, including design, control, production, and documentation, are completely freely accessible and can be adapted as desired to suit the user's own task, for example by modifying adapters for base bodies and counterbodies, integrating a reservoir for lubricants, etc. To further lower the hurdle for a reproduction, it was our goal to be able to manufacture the tribometer completely additively from frequently used plastics such as ABS or PETG, apart from inexpensive standard and purchased parts. For the programming of the control and evaluation system, we also consistently relied on open-source software solutions to be able to customize the tribological tests. We see considerable added value in this open hardware-based test rig concept, especially in the following points.

- The access to tribological measurement technology for companies and institutes is facilitated and the inhibition threshold to address tribological issues even in rare cases is lowered.
- The simultaneous use of several identical test benches increases the number of samples and thus the statistical significance of the results. This could be exciting regarding big data and machine learning approaches.
- The tests are easily comparable, and the test setup is reproducible in the best possible way.
- Several time-intensive tests, such as those on coating failure, can be carried out at the same time, which would occupy a test stand for several days to weeks in some cases.
- Due to the cost-effective design, the concept is suitable for teaching and training purposes, which can sustainably increase interest in tribological topics and their relevance.
- Round-robin tests can be easily performed on a large scale to further address measurement aspects in the tribology environment.

Within the scope of this work, in addition to the basic concept as well as its implementation, the focus is on the statistical evaluation of the tests carried out on identical samples for validation. In addition, the results from the development phase are presented to consider the significant influence of the test setup on the measurement results. For the exact design details and the components used, please refer to the design and data sets published together with this contribution [57] under a CC BY-NC-SA 4.0 license [58].

2. Materials and methods

In the following, we summarize the design concept and its constructive, metrological, and electronic implementation, as well as the programming and fabrication, based on the system requirements defined in advance. In addition, the testing conditions used for validation are defined.

2.1. System requirements

Our goal was to develop a tribometer with as simple a design as possible, which can be manufactured and operated cost-effectively and without special knowledge, even in large quantities. This resulted in the following core requirements.

- Components manufacturable exclusively with simple 3D printers using the Fused Filament Fabrication (FFF) process with common plastics (e.g., ABS, PETG), as well as inexpensive and widely used standard parts (e.g., screws) and purchased parts (stepper motor, load cell, cables, microcontrollers, etc.).
- Completely free programmable and on open-source control system.
- Easy assembly with standard tools and solderable control board.
- Easy setup and execution of the test with simple result data sets
- Tribological test conditions in basic configuration:
 - o Sliding speed up to $u = 1 \frac{\text{m}}{\text{s}}$, oscillation possible

- o Friction radius up to $r = 15 \text{ mm}$.
- o Normal force up to $F_n = 50 \text{ N}$.
- o Base body: Disc with $\varnothing 30 \text{ mm}$ and $h = 5 \text{ mm}$.
- o Counterbody: Balls with $d_b = 4 \text{ mm}$ ($\varnothing 6 \text{ mm}$, $\varnothing 8 \text{ mm}$ and $\varnothing 10.3 \text{ mm}$ adapter available)

For the basic concept, the tribometer was designed to cover the typical test conditions mentioned. However, the concept and in particular the control and measurement technology can be easily adapted to other applications and test conditions by changing the mechanical design (e.g., motors, bearings, and specimen adapters).

2.2. Metrological concept

As with all pin-on-disc tribometers, the basic concept is based on a relative motion between a stationary pin and a rotating disk (see Fig. 1 (a)). The resulting sliding velocity u can be adjusted via the speed of the motor and the friction radius r . The contact pressure can be adjusted via the diameter of the ball d_b (or pin) and the applied normal force F_n . The frictional force F_f generated in the contact in the sliding direction is measured directly by a load cell with measuring bridge. The COF present in the contact is calculated according to Coulomb's law of friction to

$$f = \frac{F_f}{F_n}. \quad (1)$$

The proven basic design was based on the pin-on-disc tribometer MT1 previously developed at LSCAD, shown in Fig. 1 (a). The load arm of the tribometer is supported at the pivot point in the bearing pedestal and can be moved to adjust the friction radius. In the unloaded condition, this is horizontal, with the center of gravity shifted to the pivot point via a balancing load F_l . The normal force F_n is applied gravimetrically directly over the contact point to exclude parasitic bending moments around the axis perpendicular to the measuring direction. Such could be determined in an early development phase (see Fig. 2(a)) with eccentric load application in sensor errors. In standard mode, a previously calibrated water-filled vessel is used. In principle, any masses are possible if the resulting center of gravity can be ensured above the contact point. For higher loads, the normal force $F_{n,alt}$ can alternatively be applied via a string with attached mass, in which case the leverage ratio must be considered. In this case, in addition to the measurement uncertainty of the precision balance used for the test load, further uncertainties are included in the load application, which reduces its accuracy and precision. Direct load application is therefore always preferable if possible. Load application with a string can lead to a shift in the effective load application point during the test due to vibrations, for example. In addition, production-related deviations in the distances and the parasitic bending moment on the load cell are further sources of error. The concept used is shown schematically in Fig. 1(b).

2.3. Mechanical structure

The entire mechanical design results from the requirement that all parts should be additively manufactured using the FFF process, which is why typical manufacturing constraints such as printing bed size and overhang angle were directly considered. The motor and the bearing pedestal, on which the tribometer's cantilever is mounted, are mounted on a stiff base platform. All other components are also mounted on the platform. The first prototypes were mounted on a wooden plate, the final assembly then on an additively manufactured platform. The final structure of the test rig and the original prototypes (TF1 and TF2_v1) are shown in Fig. 2. Within the scope of this work, five test rigs TF1 ("TriboFish" due to the shape of the leverage created for material saving reasons), TF2, TF3, TF4 and TF5 were implemented and tested.

To achieve the most stiff and direct force application possible, the plastic components were all designed to minimize the path of the force flow. The bearing pedestal was printed from solid material as this is

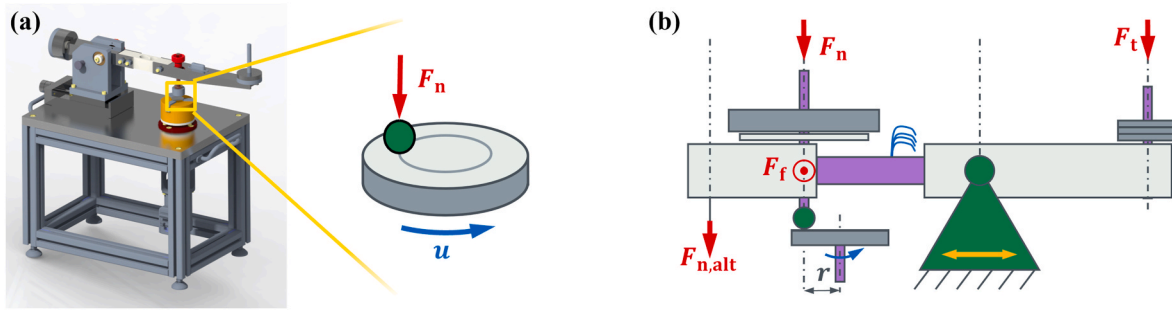


Fig. 1. Typical configuration of a pin-on-disc tribometer with contact situation (a) and simplified concept of the friction measurement (b).

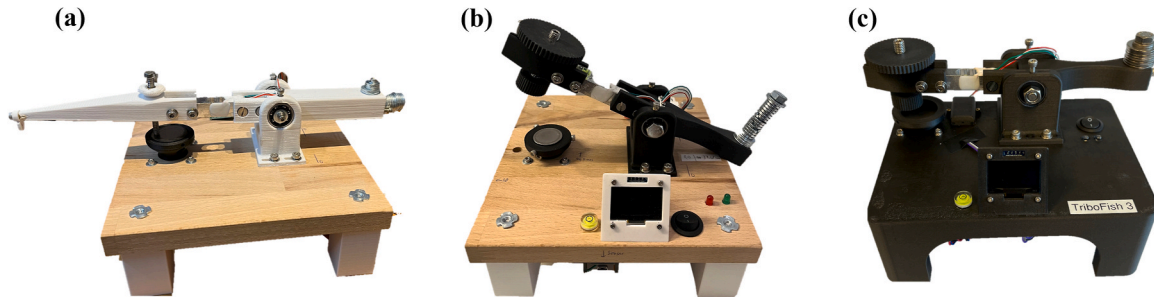


Fig. 2. Construction of the first wood-based PETG prototype TF1 (a), the improved version TF2_v1 (b) and the final fully printed design of TF2, TF3, TF4 and TF5 (c).

where the highest deformations occurred in the prototypes, which can lead to a deviation from the nominal contact position. The bearing pedestal is attached to the base plate via four slotted holes, allowing the friction radius to be adjusted. By clamping the bearings in the bearing pedestal by means of screws, the cantilever can be positioned so that the sliding direction at the contact point can be set exactly tangential to the friction circle and parallel to the measuring axis of the load cell. The stepper motor is dimensioned for a COF between $\mu = 0$ and $\mu = 1$ depending on the test setup and is stiffly connected to the base plate. The rolling bearing ball is screwed to the cantilever via an adapter, whereby the cantilever can be adjusted via the thread using a spirit level. The clamping of the disk with sufficiently good axial runout proved to be complex in the first prototypes due to the insufficient form and position deviations resulting from 3D printing. Radial clamping by means of three screws (see Fig. 2(b)) did not provide sufficient clamping in one test, which is why a decoupled clamping system (see Fig. 3) was developed with which the axial run-out of the disk can be adjusted via three screws directly against the motor shaft. The plastic thread ensures that the screws do not come loose during the test.

2.4. Control and electronics

The control and data recording should be completely open-source and microcontroller-based. All other electronic components should also be widely used standard components. Due to the wide distribution,

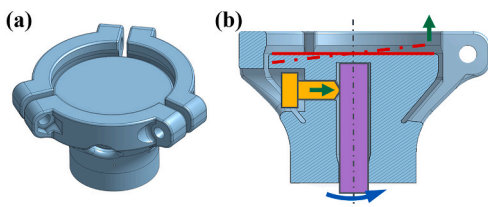


Fig. 3. Decoupled clamping adapter in 3D (a) and sectional view with schematic representation of axial runout adjustment (b).

as well as the extensive libraries and components available, ARDUINO™ Nano or equivalent microcontrollers based on the Atmega328 chip were used for the control, since their performance and pins are sufficient for the requirements and are at the same time inexpensive. The motor used was a NEMA17 stepper motor with a maximum torque of $M_{max} = 0,059$ Nm with a A4988 driver module. Due to the control of the individual steps and the limited computing capacity of the Arduino, there is a slight deviation from the set speed. In preliminary tests, a deviation in the rotational speed of a maximum of 1 % was determined by simple time measurement. However, this error is already considerably smaller than the error that can result from a deviating friction radius. Due to the single core architecture and the limited clock frequency of the chip (16 MHz), a control of the single motor steps with simultaneous evaluation of the load cell is not possible. Therefore, the system was divided into a main controller, which controls and processes the measurement, and a motor controller, which only controls the motor and is controlled by the main controller via the serial interface. The force measurement is done by a 50 N load cell in combination with a HX711 AD-converter, which samples with 10 Hz in basic configuration (can be switched to 80 Hz), whereby a chip-internal moving average filtering of the measured values is possible. The measured values are written to an SD card via an SD card module including the testing conditions used. In addition, the most important test parameters, test instructions and measured values are displayed in real time via an I2C OLED display. Two status LEDs additionally indicate the status of the current test. The tribometer is powered by a 12 V DC power source, which is required for the stepper motor. An LM2596S step down converter additionally regulates the voltage to 5 V for the microcontrollers. The tribometer is switched on and off by a toggle switch, everything else is software controlled. The circuit diagram as well as the final soldered board and its wiring with the other components of the tribometer is shown in Fig. 4.

The programming of the controllers is based on freely available open-source libraries. More detailed information can be found in the comments of the code, published at (Zenodo link with DOI will be added to the publication).

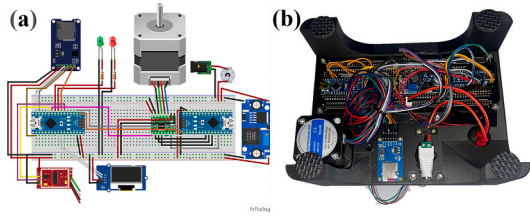


Fig. 4. Schematic circuit design (a) and its implementation in the tribometer (b).

2.5. Manufacturing and assembly

Most of the mechanical components are designed in such a way that they can be manufactured with commercially available 3D printers using the FFF process. However, additive manufacturing is also conceivable with other processes, depending on the respective manufacturing restrictions. In principle, inexpensive materials and printing systems are possible and appear to meet the requirements. The first prototypes (see Fig. 2(a)) were printed on a Prusa i3 from GEEETech using PETG with a layer height of 0.2 mm and a nozzle with a diameter of 0.5 mm. In further development, the components were then all printed on a Mark TwoTM from Markforged[®] made of OnyxTM (carbon short fiber reinforced nylon [59]) with a layer height of 0.1 mm and a nozzle diameter of 0.4 mm to make the tribometer as stiff as possible. For this reason, the bearing block and the specimen holder were printed from solid material without infill structure. All other components were printed with a triangular infill structure with filling levels between 28 % and 55 %. Here, depending on the material and printing process used, a compromise between stiffness and material usage must be found. The parts were all arranged in such a way that they could be printed in one printing process within approximately 60 h, as shown in Fig. 5.

The threads for grub screws and screws are partly already printed and must be recut afterwards. Otherwise, no further post-processing of the components was required. All other components are commercially available. The main board is assembled and soldered before starting the assembly. The load cell is also soldered to the HX711 AD converter to eliminate contact losses that would lead to measurement errors. All other components are plugged and screwed during assembly; no special equipment is required for this. Detailed assembly instructions are freely available in (Zenodo link with DOI will be added to the publication). All necessary pre-assembled components as well as the final assembly of the tribometer are shown in Fig. 6(a) and (b). It should be mentioned at this point that the load cell should be calibrated for the first-time during assembling and then checked for sufficient measuring accuracy. For this purpose, the load cell is rotated by 90° and clamped so that the weight of a test weight acts in the direction of measurement (see Fig. 6(c)). The mass used for calibration must be known with sufficient accuracy and should be in the order of magnitude of the force to be measured. We have used a weight force of $F_g = 5$ N here. Calibration should also be repeated at regular intervals after assembly. Furthermore, the linearity of the measurement should be ensured by using different test weights. The deviations of the sensor were less than 1 % compared to a precision balance in all cases examined. However, it should be noted that this procedure does not comply with the ISO 376 [60] standard and the

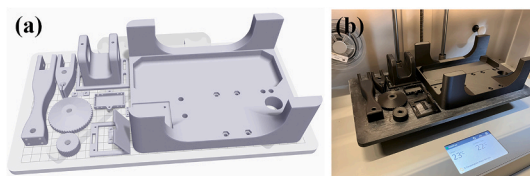


Fig. 5. Arrangement of all components in the print bed with 320 mm × 132 mm (a) as well as the printed components (b).

measurement uncertainty was not explicitly investigated.

2.6. Cost estimation

The core aspects in the development of the tribometer were a design that was as cost-effective as possible and simple assembly. The total costs for the presented assembly, including all purchased parts, can be estimated at approx. 50–150 €, depending on the manufacturing process and printing material. The material costs for the conventionally manufactured MT1 test stand were approx. 2600 € for comparison. In addition, the required manufacturing and assembly effort must be considered. Depending on experience, this can be assumed to be approx. 2–8 h, whereas the production of the MT1 took approx. 80 h.

2.7. Setup and experimental conditions

First, before each test, ensure that the load cell and the test weights used in the tribometer test have been properly calibrated. The axial runout of the specimen adapter must also be adjusted, aiming for a maximum deviation of 0.02 mm following ISO 18535:2016 [6]. The desired pin track radius is then set and checked via the diameter of the wear track on a setting disc. The contact point is adjusted via the cantilever so that the direction of friction is tangential to the pin track circle and in the direction of measurement. The cantilever is then brought into balance. The remaining test conditions are written directly to the main controller via USB before the tests and can be adapted as required within the technically possible limits of the hardware used. Conceivable are e.g., continuous sliding, oscillating tests with different swing angles as well as defined speed ramps. After switching on, all modules are initialized, and the force sensor is zeroed. Then the test force is applied, and the test starts automatically with the stored test parameters. The test stops when either the maximum sliding distance or alternatively the test time or number of revolutions is reached or when limit values for the COF have been exceeded to a defined extent. In the event of an overload, which can also be defined, the test is also aborted. The tribometer is then switched off and the data can be imported from the SD card for further evaluation. If several tests are performed in succession, the result file is simply continued with a new header. In standard configuration the friction forces are recorded with a sample rate of 10 Hz. The test conditions for the uniform tests carried out as part of this work are shown in Table 1.

As with Round Robin tests, the test conditions were selected so that all parameters except the test rig used were identical. $n = 5$ repeat tests were performed in each case. For comparison, the tests were also carried out on the MT1 tribometer. This has the identical control system and data recording. The tests with Setup 1 were first performed on the TF1 and TF2_v1 as shown in Fig. 2(b) and (c). At this stage, test rig TF2_v1 still received a bearing pedestal filled with infill structure. For reasons mentioned above, this was subsequently replaced by a fully filled print. Further tests were then carried out on the reinforced TF2 and a completely identical test rig TF3. Based on the promising results of Setup 1, the tests for Setup 2 were carried out with the four identical test benches TF2, TF3, TF4 and TF5, and comparatively with MT1. As the tests in Setup 1 were carried out during the further development of the tribometer, different configurations of the test rig were used there than in Setup 2, apart from TF2 and TF3. An overview of the differences between the individual test rigs is summarized in Table 2.

Prior to testing, the hardened specimens were plane ground on a wet grinding machine in steps with 1000, 2000 and 4000 grit to achieve a surface roughness of at least $R_a = 0.04$ μm and thus matching the order of magnitude of the counter bodies. The specimens were then cleaned in isopropanol in an ultrasonic bath for 5 min. The oil was applied before the test with a microliter pipette in droplet form (quantity 2 μl) evenly and selectively at five points on the subsequent wear track.

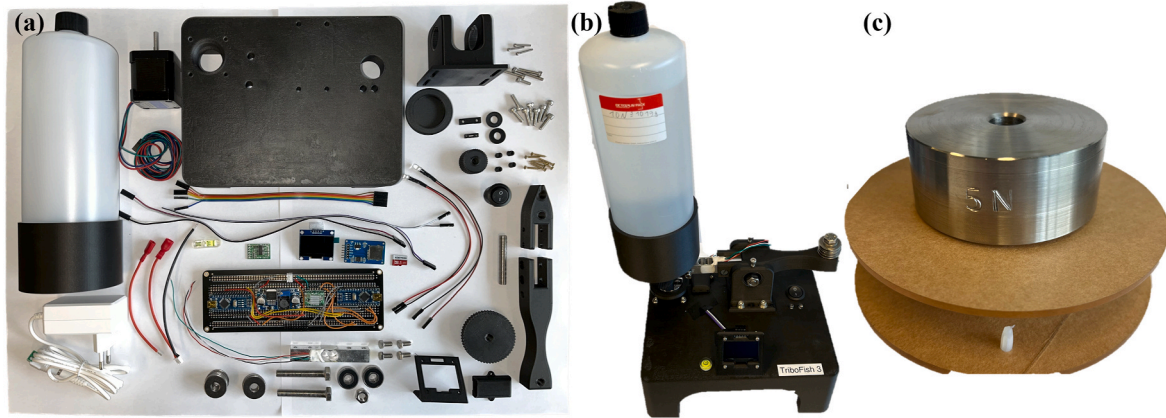


Fig. 6. Overview of the preassembled parts required (a), the final assembled tribometer TF3 (b) and the setup for load cell calibration (c).




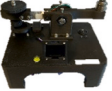
Table 1

Uniform test conditions for Setup 1 and Setup 2.

	Setup 1 ($n = 5$ per tribometer)	Setup 2 ($n = 5$ per tribometer)
Base body	Disc with $h = 5$ mm and $\varnothing 30$ mm hardened X153CrMoV12 (1.2379)	Disc with $h = 5$ mm and $\varnothing 30$ mm 17-4 P H (1.4548)
Counterbody	100Cr6 (1.3505) balls with $\varnothing 4$ mm, grade G10, DIN 5401, Ra $\leq 0,02 \mu\text{m}$, hardness ≥ 61 HRC	
Base body hardness	61.2–63.5 HRC	33.6–35.8 HRC
Base body surface R_a	0.022–0.036 μm	0.021–0.032 μm
Lubricant	10 μl CLF-65 E (RAZIOL, Germany)	10 μl PAO 40
Normal force F_n	10 N	
Hertzian pressure p_h	1861 MPa	
Sliding speed u	0.1 m/s	
Pin track radius r	10 mm	
Maximum sliding distance w	500 m	
Relative humidity	40–46 %	40–46 %
Temperature	17.0–22.0 $^{\circ}\text{C}$	20.0–24.0 $^{\circ}\text{C}$

Table 2

Building conditions of the used Tribometers compared to the final version of TF2-TF5.

Name	Design	Control and electronics	Mechanical setup
MT1		Internal AD filter in Setup 1, Identical to the final control of TF2-TF4 in Setup 2	Completely metal construction with the use of industry-standard components (Three-jaw chuck, turned and milled parts, linear guide)
TF1		Internal AD filter over 16 values	Base plate made of wood, Printed parts made of PETG, Clamping of the samples via three screws, Eccentric load application
TF2_v1		Internal AD filter over 16 values	Base plate made of wood, printed parts made of nylon with reduced rigidity, clamping of the samples via three screws
TF2-TF5		Final version	Final version

2.8. Analysis methodology and statistics

To determine the equality of the test conditions, the Rockwell hardness (HRC, DuraJet10G5, ZwickRoell, Germany) and roughness (MarSurf PS10, Mahr, Germany) of all specimens were determined. The actual diameter of the wear track was determined as a deviating parameter of the test rigs on the optical microscope (Metallux I, Leica, Germany). The diameter was measured as the mean value between the inner and outer edge of the wear track. The wear diameter of the counterbody was also determined on the optical microscope. The COF curves, and the time average were evaluated with Python based on the stored measured values, whereby individual outliers in the form sensor errors were excluded. In the first test series on MT1, TF1 and TF2_v1, additional moving average filtering was performed within the AD converter over 16 measured values. For the following tests, the original values were filtered in the same way using Python. However, for the mean COF, the evaluation is identical. The corresponding scripts are provided in (Zenodo link with DOI will be added to the publication).

The statistical evaluation of the tests is based on the typical procedure for a classic measurement system analysis. Here, repeatability indicates how large the variance is for identically repeated tests on a single test bench. In contrast to the measurement of a calibrated standard in metrological systems, the deviations caused by the tribological contact itself are included in tribological testing. Thus, the determination of repeatability in destructive tests is strictly speaking not possible, which is why it is defined below as reproducibility per tribometer. The overall reproducibility describes how large the variance in the tests is between the individual test stands. This is expressed as a relative standard deviation of the mean friction or wear. In addition, a statistical pairwise comparison is performed between all groups in each setup to check whether significant differences can be detected. Due to the small sample size of $n = 5$ per group, this is carried out in addition to the two-sided t -test for unpaired samples using a non-parametric Wilcoxon rank sum test with the Python package `scipy.stats.ranksums` (see e.g. Ref. [61]). The significance level $p = 0.05$ was used.

3. Results and discussion

The following is a summary of the results of the measurements carried out for the validation of the developed tribometer.

3.1. Comparability of the test conditions

The hardness of the discs is between 61 HRC and 64 HRC for all specimens. The surface roughness measured at three points per specimen is in the range of $R_a = 0.021 \mu\text{m}$ and $R_a = 0.036 \mu\text{m}$ for all specimens. The specimens can thus be considered sufficiently comparable.

The humidity varied in a range of 40%–46 %. The room temperature was 17.0–22.0 °C for the Setup 1 and 20.0–24.0 °C for the Setup 2. The environmental conditions during the tests can therefore also be considered comparable. The diameters of the wear tracks measured after the tests are shown in Fig. 7. The maxima and minima are used in the following in all figures, since the range of values seems to be statistically more suitable for a small sample than the frequently used standard deviation.

The subsequently measured diameters deviate slightly from the set nominal (pin track) diameter of 20 mm. This is mainly since the printed components still distort minimally when the bearing block is tightened, and the printed ball holder also introduces a certain positioning error when tightened. Additionally, even small deviations of the cantilever from the horizontal will result in a deviating measured radius. Once the pin track radius for a test rig has been set, however, the deviations between the repeat tests are significantly smaller. Since the radius only has a linear effect on the nominal speed, and this has no influence on the set normal force or the measured friction force, the error for the test conditions can be classified as rather small compared to other random influences deriving from the test.

3.2. Results of setup 1

Fig. 8 shows the curves of the COF for all 25 repeated measurements of Setup 1, plotted against the sliding distance. For better readability, the ordinate axis is shown shortened. Although somewhat exaggerated by the axis shift, it is noticeable that the highest deviation in the curves of the COF is present in the first two rows TF1 and TF2_v1. This applies both between the repeated measurements and between the test rigs. An outlier can be seen at TF1. This is since the specimen came loose in the holder during one measurement. For the reference test rig MT1, the curves of the individual measurements differ in a similar order of magnitude. The curves of the revised and identical test rigs TF2 and TF3, on the other hand, are almost identical and the difference between the two tribometers also appears to be smaller than between the individual repeated measurements of each.

The COF averaged over the sliding distance are shown in Fig. 9(a).

The mean values indicate similar findings as in the curves over time (sliding distance). Even with the first prototypes and the reference test rig, differences between the individual repeat measurements are of a similar magnitude to the differences between the test rigs. This suggests that all test rigs are suitable in principle for measuring tribological behavior in the case of Setup 1. The measurement results for the identical test rigs TF_2 and TF_3, on the other hand, are almost identical. The Null hypothesis for the statistic evaluation is, that the friction means of both independent samples come from the same distribution. This hypothesis cannot be rejected at the 5 % significance level with a p -value of 0.117. If the same test is performed with TF3 and TF2_v1, for example,

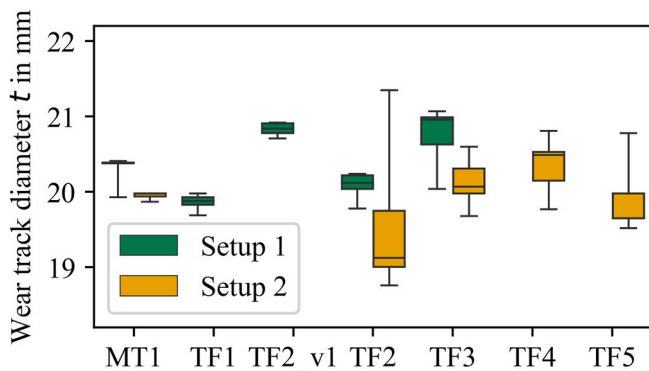


Fig. 7. Resulting wear track diameter of the individual tribometers in Setup 1 and Setup 2 ($n = 5$). It should be noted that not all configurations were used in both setups. The cut of ordinate axis should be noted.

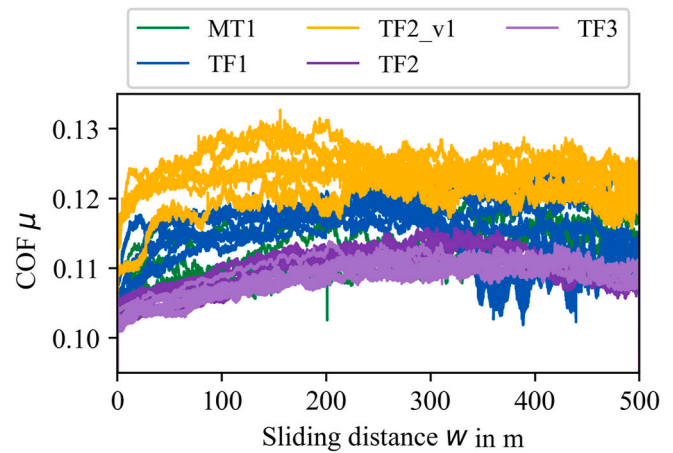


Fig. 8. Curves of the COF over the sliding distance for all 25 tests of Setup 1 using moving average smoothing with 1.6 s filter size. The cut of ordinate axis should be noted.

the hypothesis must be rejected with a p -value of 0.009. The t -test confirms this result even more clearly.

The wear of the counterbodies is shown in Fig. 9(b). Here it can be clearly seen that the variance in the results for MT1, TF1 and TF2_v1 is significantly greater than for the final test rigs. The differences between the repeated tests are already in part significantly greater than between the individual test rigs. The statistical evaluation based on the aforementioned tests shows that the wear results between the identical test stands TF2 and TF3 do not differ significantly. At the same time, however, the results also show very clearly that the friction and wear characteristics determined are significantly different, even if the test rigs differ only slightly (e.g., TF_2 and TF_2_v1).

In conclusion, the test rig developed in the final configuration has a very good reproducibility of 0.4 % in terms of mean friction and 0.6 % in terms of mean wear. This is thus significantly lower than the reproducibility per tribometer for each of the two test benches, with up to 0.6 % in friction and up to 5.1 % in wear. The relatively good reproducibility per tribometer (cf. e.g. with [31]) can presumably be explained by the fact that similar mixed friction conditions occurred in all tests and the variance of the tribological contact itself was lower.

3.3. Results of setup 2

More complex contact conditions resulted for the second tribosystem (Setup 2) studied. At the beginning of the tests, elasto-hydrodynamic lubrication conditions were present, which changed to mixed lubrication after varying run-in behavior. This can be seen clearly from the sudden change in COF curves in Fig. 10.

To further evaluate the reproducibility of the test rig, two additional identical test rigs TF4 and TF5 were used for the measurement in addition to the conventional MT1 and the two test rigs TF2 and TF3. While mainly elasto-hydrodynamic lubrication was present throughout in 4 of 5 tests on the MT1 (cf. Fig. 10), the four identical test rigs showed very similar tribological behavior. The statistical evaluation of the friction and wear behavior is summarized in Fig. 11.

Regarding friction, there are no significant (Wilcoxon and t -test) differences between the four test stands, at the same time the difference to the MT1 results is highly significant. Regarding wear, the same conclusions can be drawn. It is assumed that the different design of the MT1 in this case led to minimally changed contact conditions (e.g., vibrations, mass inertia, etc.), which, however, made the decisive difference as to whether mixed lubrication was present (for MT1 only at one outlier in Fig. 11) in the contact or not. This shows that the test rig used is of considerable importance, especially for complex or unstable contact conditions, and that results can hardly be reproduced on different

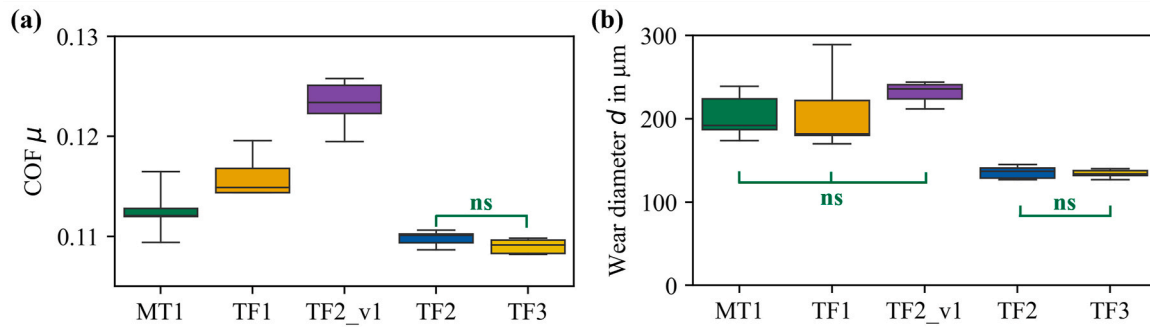


Fig. 9. COF of the individual test rigs averaged over the sliding distance (a) and the associated diameter of the wear calotte of the counterbody (b) for Setup 1 with given non-significant (ns) differences between the groups.

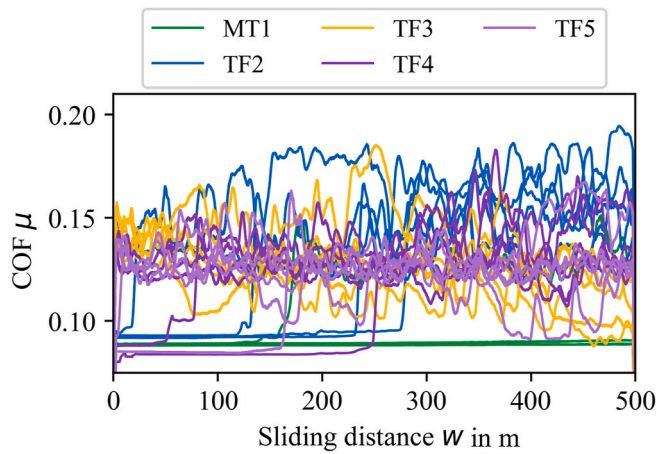


Fig. 10. Curves of the COF over the sliding distance for all 25 tests of Setup 2 using moving average smoothing with 50 s filter size. The cut of ordinate axis should be noted.

tribometers. Also, in Setup 2, the test rigs TF3, TF4 and TF5 show outstanding reproducibility with 1.2 % for friction and 0.97 % for wear. The TF2 test rig was excluded in this case, as individual tests had to be repeated there due to a loose contact in the board and the resulting faulty recording, and thus the repeated tests were not performed simultaneously. Due to the unstable contact conditions, the variance is higher overall, and the reproducibility per tribometer was between 6.0 % and 7.7 % for friction and between 6.4 % and 16.1 % for wear.

4. Conclusions

Within the scope of our work, we have presented an open hardware based tribometer kit and successfully validated its measurement

capability by means of two different tribological test setups. We succeeded in developing a freely customizable and easy-to-manufacture test rig that nevertheless measures at the level of typical self-developed test rigs, or even exceeds it in the cases presented. It could be shown that all results regarding friction and wear can be reproduced very well on several identical test rigs. The overall reproducibility was significantly better than the reproducibility per tribometer, which is mainly influenced by the tribological system itself. Theoretically, this makes it possible to carry out comparable repeated tests on several identical test rigs, which means that the number of tests can be scaled up considerably. On the other hand, however, it has also been shown that tests on one tribometer cannot be reproduced on other tribometers (e.g. MT_1 and TF). This is not necessarily relevant in practice, as long as only relative comparisons (e.g. different materials) are carried out on the same test rig, but it is impossible to compare the results with other published results, for example. The following important findings can be summarized.

- In the final development stage, the repeated tests showed a smaller deviation in the friction and wear evaluation than with the MT1 reference test rig.
- In the case of identical builds, the results obtained are directly comparable without significant differences, the influence of the specimen and the test itself being greater than that of the test rig used.
- The reproducibility of the measured values was 0.4 % and 1.1 % for friction and 0.6 % and 1.0 % for wear between the identical test rigs.
- The reproducibility per tribometer was up to 7.7 % and 16.1 % for friction and wear, respectively, which means that the influence of the individual specimens can be considered significantly greater than that of the test rig.
- It was confirmed that the tribological test setup and test rig has a significant influence and is decisive for the reproducibility of the tests.

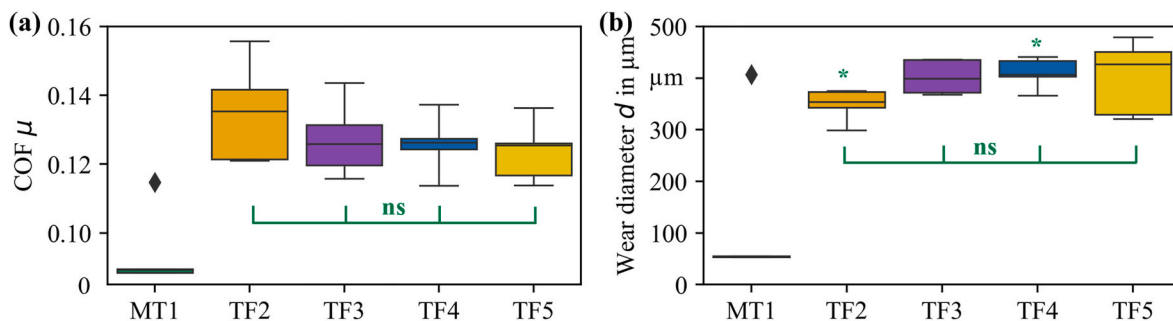


Fig. 11. COF of the individual test rigs averaged over the sliding distance (a) and the associated diameter of the wear calotte of the counterbody (b) for Setup 2 with given non-significant (ns) differences and the only significant (*) difference between the groups.

The investigations show that the subject of measurement uncertainty in tribometer tests has so far still been neglected in most studies. Due to the extremely complex and diverse influences, it is hardly possible to consider individual error influences completely separately from one another, but it seems sensible to investigate them further not only for the test rig presented here, but also in general. For a better statistical evaluation and a determination of the measurement uncertainty in accordance with the GUM, a high number of tests is decisive. For instance, the influence of axial runout, pin track radius or vibration behavior in the test would be interesting. The long-term goal of our research is the development of a uniform standard that can then be used to specify the reproducibility of tribological testing in a uniform and comprehensible manner. The presented tribometer can be used, for example, to perform tests with a high throughput and thus to detect systematic correlations, e.g., in combination with machine learning approaches. Another potential use is in teaching.

Statement of originality

We confirm that the work described has not been published previously, that it is not under consideration for publication elsewhere, that its publication is approved by all authors and tacitly or explicitly by the responsible authorities where the work was carried out, and that, if accepted, it will not be published elsewhere in the same form, in English or in any other language, including electronically without the written consent of the copyright-holder.

Funding

This research received no external funding.

CRedit authorship contribution statement

Christian Orgeldinger: Writing – original draft, Validation, Software, Resources, Methodology, Investigation, Formal analysis, Data curation, Conceptualization. **Tobias Rosnitschek:** Writing – review & editing. **Stephan Tremmel:** Writing – review & editing, Resources, Methodology.

Declaration of competing interest

The authors declare that they have no known competing financial interests or personal relationships that could have appeared to influence the work reported in this paper.

Data availability

In line with the Open Hardware approach presented in this paper, all data including CAD models, codes, wiring diagrams and an English-language assembly instruction and manual are made available under <https://doi.org/10.5281/zenodo.11580760>.

Acknowledgments

The authors greatly acknowledge the continuous support of the University of Bayreuth. Furthermore, we would like to thank Julian Kämpmann for the support during the repeated measurements.

References

- [1] K. Holmberg, A. Erdemir, Influence of tribology on global energy consumption, costs and emissions, *Friction* 5 (2017) 263–284, <https://doi.org/10.1007/s40544-017-0183-5>.
- [2] T. Mang, K. Kobzin, T. Bartels, *Industrial Tribology: Tribosystems, Friction, Wear and Surface Engineering, Lubrication*, Wiley-VCH, Weinheim, 2011.
- [3] G02 Committee, Test Method for Wear Testing with a Pin-On-Disk Apparatus, ASTM International, 2017, <https://doi.org/10.1520/G0099-17>.
- [4] G02 Committee, Test Method for Linearly Reciprocating Ball-on-Flat Sliding Wear, ASTM International, 2022, <https://doi.org/10.1520/G0133-05R16>.
- [5] D.I.N. Tribologie, Prüfung von Reibung und Verschleiß; Modellversuche bei Festkörpergleitreibung, Kugel-Scheibe-Prüfsystem, 1992.
- [6] ISO, *Diamond-Like Carbon Films — Determination of Friction and Wear Characteristics of Diamond-like Carbon Films by Ball-On-Disc Method*, 2016.
- [7] F04 Committee, Test Method for Wear Testing of Polymeric Materials Used in Total Joint Prostheses, ASTM International, 2017, <https://doi.org/10.1520/F0732-17>.
- [8] D. Meresse, M. Siroux, M. Watremez, S. Harmand, L. Dubar, Estimation of Three-Dimensional Distribution of Heat Flux on the Pin Frictional Surface during a Pin on Disc Test, 2011, pp. 1137–1142, <https://doi.org/10.1063/1.3589669>. Belfast, (United Kingdom).
- [9] J. Wahlström, A pin-on-disc tribometer study of friction at low contact pressures and sliding speeds for a disc brake material combination, *Results in Engineering* 4 (2019) 100051, <https://doi.org/10.1016/j.rineng.2019.100051>.
- [10] B. Rothhammer, M. Schwendner, M. Bartz, S. Wartzack, T. Böhm, S. Krauß, et al., Wear mechanism of superhard tetrahedral amorphous carbon (ta-C) coatings for biomedical applications, *Adv. Mater. Interfac.* 10 (2023) 2202370, <https://doi.org/10.1002/admi.202202370>.
- [11] Y. Zhou, Y. Tian, S. Meng, S. Zhang, X. Xing, Q. Yang, et al., Open-source tribometer with high repeatability: development and performance assessment, *Tribol. Int.* 184 (2023) 108421, <https://doi.org/10.1016/j.triboint.2023.108421>.
- [12] A. Seynstahl, S. Krauß, E. Bitzek, B. Meyer, B. Merle, S. Tremmel, Microstructure, mechanical properties and tribological behavior of magnetron-sputtered MoS₂ solid lubricant coatings deposited under industrial conditions, *Coatings* 11 (2021) 455, <https://doi.org/10.3390/coatings11040455>.
- [13] P. Wu, C. Zhang, J. Luo, Design and build of a micro-tribometer with high vacuum and low temperature, in: T. Uhl (Ed.), *Advances in Mechanism and Machine Science*, vol. 73, Springer International Publishing, Cham, 2019, pp. 3789–3794, https://doi.org/10.1007/978-3-030-20131-9_375.
- [14] H. Kumar, S. Vijayaraghavan, S.K. Albert, A.K. Bhaduri, K.K. Ray, Design and development of high-temperature tribometer for material testing in liquid sodium environment, *IJNEST* 10 (2016) 276, <https://doi.org/10.1504/IJNEST.2016.078962>.
- [15] Krauss PG, Awtar PS. Multi-Function Tribometer Design n.d.
- [16] Lin Z-J. Design of a Tribometer to Study Friction in Threaded Fastener Interfaces. n.d.
- [17] DA-Lippmann Konstruktion eines Stift-Scheibe-Prüfstands, 1992 n.d.).
- [18] N. Marjanovic, B. Tadic, B. Ivkovic, S. Mitrovic, Design of modern concept tribometer with circular and reciprocating movement, *Tribology in Industry* 28 (2006).
- [19] T.J. Joyce, Biopolymer wear screening rig validated to ASTM F732-00 and against clinical data, *Tribol. Mater. Surface Interfac.* 1 (2007) 63–67, <https://doi.org/10.1179/175158407X181480>.
- [20] C.B. Mohan, C. Divakar, K. Venkatesh, K. Gopalakrishna, K.S. Mahesh Lohith, T. N. Naveen, Design and development of an advanced linear reciprocating tribometer, *Wear* 267 (2009) 1111–1116, <https://doi.org/10.1016/j.wear.2009.01.047>.
- [21] E. Ochs, P. Iglesias Victoria, Systems, Design, and Complexity, Graduation Design Project: Designing and Building a Pin-On-Disk Tribometer, vol. 11, American Society of Mechanical Engineers, Houston, Texas, USA, 2015, <https://doi.org/10.1115/IMECE2015-51148>. V011T14A026.
- [22] Z. Chen, J. Hillairet, V. Turq, Y. Song, Q. Yang, G. Lombard, et al., Multifunctional tribometer development and performance study of CuCrZr-316L material pair for ITER application, *Tribol. Int.* 116 (2017) 208–216, <https://doi.org/10.1016/j.triboint.2017.07.024>.
- [23] H. Singh, A.K. Singh, Y.K. Singla, K. Chattopadhyay, Design & development of a low cost tribometer for nano particulate lubricants, *Mater. Today: Proc.* 28 (2020) 1487–1491, <https://doi.org/10.1016/j.matpr.2020.04.826>.
- [24] L.P. Alvizo, Y.L.R. Acosta, J.R.P. Martínez, Dr. Demófilo Maldonado cortés, dra. Laura Peña parás. Reciprocating sliding motion tribometer design. *Proceedings of the International Conference on Industrial Engineering and Operations Management, Monterrey, Mexico, November*.
- [25] K. Berglund, M. Rodiouchkina, J. Hardell, K. Kalliorinne, J. Johansson, A novel reciprocating tribometer for friction and wear measurements with high contact pressure and large area contact configurations, *Lubricants* 9 (2021) 123, <https://doi.org/10.3390/lubricants9120123>.
- [26] B.D.A. Hidalgo, V.C. Erazo-Chamorro, D.B.P. Zurita, E.A.L. Cedeño, G.A. M. Jimenez, R.P. Arciniega-Rocha, et al., Design of pin on disk tribometer under international standards, in: B.B.V.L. Deepak, D.R.K. Parhi, B.B. Biswal, P.C. Jena (Eds.), *Applications of Computational Methods in Manufacturing and Product Design*, Springer Nature Singapore, Singapore, 2022, pp. 49–62, https://doi.org/10.1007/978-981-19-0296-3_6.
- [27] I.A. Lyashenko, V.L. Popov, R. Pohrt, V. Borysiuk, High-precision tribometer for studies of adhesive contacts, *Sensors* 23 (2023) 456, <https://doi.org/10.3390/s23010456>.
- [28] J.B. De Faria, R.N.L. De Oliveira, R.M.A. Dutra, Tarsis Barbosa, DIY Tribometer: Open Source and 3D Printed Design, 2018, <https://doi.org/10.13140/RG.2.2.16447.64167>.
- [29] E11 Committee. Practice for Conducting an Interlaboratory Study to Determine the Precision of a Test Method. ASTM International; n.d. <https://doi.org/10.1520/E0691-23>.
- [30] H. Czichos, S. Becker, J. Lexow, Multilaboratory tribotesting: results from the versailles advanced materials and standards programme on wear test methods, *Wear* 114 (1987) 109–130, [https://doi.org/10.1016/0043-1648\(87\)90020-2](https://doi.org/10.1016/0043-1648(87)90020-2).

- [31] H. Czichos, S. Becker, J. Lexow, International multilaboratory sliding wear tests with ceramics and steel, *Wear* 135 (1989) 171–191, [https://doi.org/10.1016/0043-1648\(89\)90104-X](https://doi.org/10.1016/0043-1648(89)90104-X).
- [32] H. Czichos, K.-H. Habig (Eds.), *Tribologie-Handbuch: Tribometrie, Tribomaterialien, Tribotechnik*, Springer Fachmedien Wiesbaden, Wiesbaden, 2020, <https://doi.org/10.1007/978-3-658-29484-7>.
- [33] M. Woydt, J. Ebrecht, Influence of test parameters on tribological measurements - results from international round robin tests, *Tribotest* 10 (2003) 59–76, <https://doi.org/10.1002/tt.3020100106>.
- [34] Goldstein MA. Uncertainty Analysis of a Multifunctional Tribometer n.d.
- [35] C. Liguori, A. Ruggiero, D. Russo, P. Sommella, Accurate measurement of dry friction coefficient using reciprocating tribometer, in: 2018 IEEE International Instrumentation and Measurement Technology Conference (I2MTC), IEEE, Houston, TX, USA, 2018, pp. 1–6, <https://doi.org/10.1109/I2MTC.2018.8409747>.
- [36] C. Liguori, A. Ruggiero, D. Russo, P. Sommella, A statistical approach for improving the accuracy of dry friction coefficient measurement, *IEEE Trans. Instrum. Meas.* 68 (2019) 1412–1423, <https://doi.org/10.1109/TIM.2019.2905755>.
- [37] G.D. Leo, C. Liguori, A. Ruggiero, D. Russo, P. Sommella, Accurate measurement of Kinetic Friction Coefficient by using two types of tribometer, in: 2019 IEEE International Instrumentation and Measurement Technology Conference (I2MTC), IEEE, Auckland, New Zealand, 2019, pp. 1–6, <https://doi.org/10.1109/I2MTC.2019.8827060>.
- [38] A. Ruggiero, R. D'Amato, R. Calvo, P. Valašek, N. Ungureanu, Measurements of the friction coefficient: discussion on the results in the framework of the time series analysis, in: S. Hloch, D. Kličová, G.M. Krolczyk, S. Chattopadhyaya, L. Ruppenthalová (Eds.), *Advances in Manufacturing Engineering and Materials*, Springer International Publishing, Cham, 2019, pp. 443–455, https://doi.org/10.1007/978-3-319-99353-9_47.
- [39] D. Godfrey, Friction oscillations with a pin-on-disc tribometer, *Tribol. Int.* 28 (1995) 119–126, [https://doi.org/10.1016/0301-679X\(95\)92701-6](https://doi.org/10.1016/0301-679X(95)92701-6).
- [40] J. Prost, G. Boidi, T. Lebersorger, M. Varga, G. Vorlauffer, Comprehensive review of tribometer dynamics-Cycle-based data analysis and visualization, *Friction* 10 (2022) 772–786, <https://doi.org/10.1007/s40544-021-0534-0>.
- [41] Vale JL. Do, C.H. Da Silva, Kinetic friction coefficient modeling and uncertainty measurement evaluation for a journal bearing test apparatus, *Measurement* 154 (2020) 107470, <https://doi.org/10.1016/j.measurement.2020.107470>.
- [42] R. Novak, T. Polcar, Tribological analysis of thin films by pin-on-disc: evaluation of friction and wear measurement uncertainty, *Tribol. Int.* 74 (2014) 154–163, <https://doi.org/10.1016/j.triboint.2014.02.011>.
- [43] ISO/ICE, Messunsicherheit - Teil 3: Leitfaden zur Angabe der Unsicherheit beim Messen, 2008.
- [44] T.L. Schmitz, J.E. Action, D.L. Burris, J.C. Ziegert, W.G. Sawyer, Wear-rate uncertainty analysis, *J. Tribol.* 126 (2004) 802–808, <https://doi.org/10.1115/1.1792675>.
- [45] T.L. Schmitz, JEZiegert Action, J.C. And, W.G. Sawyer, The difficulty of measuring low friction: uncertainty analysis for friction coefficient measurements, *J. Tribol.* 127 (2005) 673–678, <https://doi.org/10.1115/1.1843853>.
- [46] B.A. Krick, W.G. Sawyer, A little analysis of errors in friction for small wear tracks, *Tribol. Lett.* 39 (2010) 221–222, <https://doi.org/10.1007/s11249-010-9605-5>.
- [47] D.L. Burris, W.G. Sawyer, Addressing practical challenges of low friction coefficient measurements, *Tribol. Lett.* 35 (2009) 17–23, <https://doi.org/10.1007/s11249-009-9438-2>.
- [48] D.L. Burris, W.G. Sawyer, Measurement uncertainties in wear rates, *Tribol. Lett.* 36 (2009) 81–87, <https://doi.org/10.1007/s11249-009-9477-8>.
- [49] D. Sheng, Y. Liu, C. Sun, J. An, Z. Gao, H. Yu, et al., Mathematical analyses and experimental verification of elimination of measurement error in UMT-2 rotating friction system, *Measurement* 208 (2023) 112401, <https://doi.org/10.1016/j.measurement.2022.112401>.
- [50] A. Bhattacharjee, N.T. Garabedian, C.L. Evans, D.L. Burris, Traceable lateral force calibration (TLFC) for atomic force microscopy, *Tribol. Lett.* 68 (2020) 111, <https://doi.org/10.1007/s11249-020-01349-y>.
- [51] R.S. Colbert, B.A. Krick, A.C. Dunn, J.R. Vail, N. Argibay, W.G. Sawyer, Uncertainty in pin-on-disk wear volume measurements using surface scanning techniques, *Tribol. Lett.* 42 (2011) 129–131, <https://doi.org/10.1007/s11249-010-9744-8>.
- [52] G. Maculotti, E. Goti, G. Genta, L. Mazza, M. Galetto, Uncertainty-based comparison of conventional and surface topography-based methods for wear volume evaluation in pin-on-disc tribological test, *Tribol. Int.* 165 (2022) 107260, <https://doi.org/10.1016/j.triboint.2021.107260>.
- [53] G. Maculotti, G. Genta, D. Quagliotti, H.N. Hansen, M. Galetto, Comparison of methods for management of measurement errors in surface topography measurements, *Procedia CIRP* 118 (2023) 1084–1089, <https://doi.org/10.1016/j.procir.2023.06.186>.
- [54] G. Maculotti, E. Goti, G. Genta, G. Marchiandi, A. Mura, L. Mazza, et al., Effect of track geometry on the measurement uncertainty of wear in pin-on-disc tribological test. *Proceedings of the 21st International Conference of the European Society for Precision Engineering and Nanotechnology*, Online, 2021, pp. 293–296.
- [55] G. Genta, G. Maculotti, Uncertainty evaluation of small wear measurements on complex technological surfaces by machine vision-aided topographical methods, *CIRP Annals* 70 (2021) 451–454, <https://doi.org/10.1016/j.cirp.2021.04.057>.
- [56] P. Pawlus, R. Reizer, Profilometric measurements of wear scars: a review, *Wear* 534–535 (2023) 205150, <https://doi.org/10.1016/j.wear.2023.205150>.
- [57] C. Orgeldinger, Open Hardware Tribometer “Tribofish” [Data set], Zenodo, <https://doi.org/10.5281/zenodo.11580760>.
- [58] N.T. Garabedian, A. Bhattacharjee, M.N. Webster, G.L. Hunter, P.W. Jacobs, A. R. Konicek, et al., Quantifying, locating, and following asperity-scale wear processes within multiasperity contacts, *Tribol. Lett.* 67 (2019) 89, <https://doi.org/10.1007/s11249-019-1203-6>.
- [59] Creative commons — attribution-NonCommercial-ShareAlike 4.0 international — CC BY-NC-sa 4.0 n.d. <https://creativecommons.org/licenses/by-nc-sa/4.0/>. (Accessed 29 June 2023).
- [60] Markforged CompositesV5.1_de.pdf n.d. https://s3.amazonaws.com/mf.product.doc.images/Datasheets/Translations/DE/Markforged_CompositesV5.1_de.pdf (accessed June 15, 2023).
- [61] DIN EN ISO 376:2011-09, Metallische Werkstoffe.- Kalibrierung der Kraftmessgeräte für die Prüfung von Prüfmaschinen mit einachsiger Beanspruchung (ISO 376:2011); Deutsche Fassung EN ISO_376:2011 n.d. <https://doi.org/10.31030/1751519>.